Electron Spin Resonance Studies of Lipid–Gramicidin Interactions Utilizing Oriented Multibilayers

Hisao Tanaka[†] and Jack H. Freed*

Baker Laboratory of Chemistry, Cornell University, Ithaca, New York 14853 (Received: July 9, 1984; In Final Form: October 23, 1984)

Macroscopically well-aligned lipid (DPPC) samples of ≤10 wt % water, which contain 0–4 mol % of the polypeptide gramicidin A (GA) and which yield reproducible ESR spectra from spin-labeled lipids and from cholestane probe, have been prepared by a recently developed method. The effect of GA was analyzed in detail by first subjecting the extensive ESR spectra obtained to the methods of spectral analysis previously developed by Freed and co-workers. The great value of combining studies on oriented samples with such quantitative theoretical analysis is emphasized. In the gel phase a heterogeneity was found, which could be analyzed as two types of regions: one of the bulk lipids and one of boundary or disordered lipids. The principal difference between the two is the greatly reduced ordering of the latter, but with little difference in fluidity. For low concentration of GA (and 7 wt % water), it is estimated that there are 60–80 disordered lipids per GA dimer, or a disordered region in the bilayer extending radially about three lipid molecules. The disordered region is reduced by increased weight percent water but does not appear to be affected by temperature. In the liquid crystalline phase the heterogeneity is no longer evident in the ESR spectra. Instead the ordering of all the lipids is significantly reduced by the addition of GA, but motional rates are only slightly reduced. In the high-temperature, low-ordering phase previously studied, addition of GA actually increases the ordering. It is concluded from these results that the principal lipid–GA interaction is that of a boundary effect such that the GA induces disorder in low-temperature and low-water-content lipids but it induces order for high-temperature and high-water-content (i.e., less ordered) lipids. It has only slight effects on lipid fluidity, in general reducing only slightly the rates of rotational reorientation. No spectral features usually attributed to "immobilized" lipids were observed in the spectra from the well-aligned samples even when they were present in spectra from dispersions of the same material content at the highest GA concentrations. If these spectral features are interpreted as associated with "trapped lipids" due to aggregation of polypeptide, then it follows that the well-aligned samples do not permit such aggregation. These results also clearly show that the heterogeneity induced by GA at very low concentrations is a distinctly different phenomenon from the one usually assigned to "immobilized" or "trapped" lipids.

I. Introduction

A current question of considerable interest is the effect of macromolecules, in the form of proteins or of polypeptides, on the structure and fluidity of lipid bilayers. While pure lipid bilayers may be considered to have liquid crystalline properties such that the lipid molecules are well oriented yet fluid, the inclusion of macromolecules may be expected to upset these features. Such matters are particularly important in understanding the physical properties of biological membranes.

Many physical techniques have been brought to bear in the study of protein–lipid and polypeptide–lipid interactions, and magnetic resonance has been one of the most prominent.[1-5] Numerous ESR studies with spin probes have led to a model of a boundary layer of lipids coating the protein molecules.[3-5] This model is based on the frequent observation that the ESR spectra have the appearance of two superimposed ESR spectra, which is usually interpreted in terms of a population of "fluid" lipids and a population of "immobilized" boundary lipids. These observations are usually made in the regime where these are not many lipid molecules per added protein or polypeptide molecule. The NMR results typically do not show such features and were initially regarded as inconsistent with a distinct boundary layer. More recently, however, researchers have invoked the idea that, since ESR explores much shorter time scales than NMR, it could be that immobilized and fluid lipids exchange on a time scale that is too fast for NMR but slow on the ESR time scale.[4,6] Thus, NMR would only show a single average set of properties for the lipids.

Recently Meirovitch et al.[7] have provided a detailed study of simulations of ESR spectra that one may expect from model membrane systems wherein there is appreciable submicroscopic (i.e., molecular) ordering and fluidity of the lipids. Since practically all the experimental studies on protein (polypeptide) interaction have been on macroscopically unoriented or dispersion samples, these workers have calculated such spectra for micro-

scopic order but with macroscopic disorder (i.e., the MOMD model). They find that in many cases they are able to reproduce the detailed shape of ESR spectra, previously interpreted in terms of the two-site model, by the use of a single-site model wherein the effect of adding protein or of lowering the temperature is modeled by increasing the ordering while decreasing somewhat the motional rates. These authors conclude that in the analysis of ESR spectra from dispersions there is sufficient ambiguity such that it is "reasonable to suspect that the one-site model is more appropriate for some cases, while other cases are better characterized by a two (or greater) site model." They emphasize the importance of (1) "careful simulation of the ESR spectra based upon well-conceived microscopic models" and (2) "carefully designed experiments to distinguish amongst them".

The present work was undertaken in the spirit of these comments. It is well-known that the use of well-oriented multilayers of liquid crystals or of lipids will lead to greatly increased spectral resolution over spectra from dispersion samples, as well as greatly increased data, in the form of spectra obtained as a function of θ, the angle between the dc magnetic field and the normal to the bilayers. When such experiments are combined with careful spectral analyses in terms of well-defined microscopic models, then one may obtain extensive insight into the molecular structure and dynamics of these oriented phases as has been amply demonstrated,

(1) D. Chapman, J. C. Gomez-Fernandez, and F. M. Goni, *FEBS Lett.* **98**, 211 (1979).

(2) J. Seelig and A. Seelig, *Q. Rev. Biophys.* **13**, 19 (1980).

(3) D. Marsh in "Membrane Spectroscopy", E. Grell, Ed., Springer-Verlag, West Berlin, 1981.

(4) P. F. Devaux in "Biological Magnetic Resonance", L. J. Berliner and J. Reuben, Eds., Plenum Press, New York, 1983.

(5) O. H. Griffith and P. C. Jost in "Spin Labeling—Theory and Applications", L. J. Berliner, Ed., Academic Press, New York, 1976, Chapter 12.

(6) M. R. Paddy, F. W. Dahlquist, J. H. Davis, and M. Bloom, *Biochemistry*, **20**, 3152 (1981).

(7) E. Meirovitch, A. Nayeem, and J. H. Freed, *J. Phys. Chem.*, **88**, 3454 (1984).

[†] Permanent address: Josai University, Saitama, Japan.

in both thermotropic[8] and lipid systems[9,10] in recent work.

It was the objective of this work to extend our ESR studies of oriented pure lipids[10] to include the effects of macromolecules. Except for early work by Smith and co-workers on orienting protein-containing membranes,[11] there has been virtually no effort of this type. Furthermore, the full power of current theoretical methods[8] has only recently been applied to the study of lipids by ESR.[9,10] In this study we examine the effect of the polypeptide gramicidin A (GA) on the phospholipid dipalmitoyl-phosphatidylcholine (DPPC), which we have already studied in some detail.[9,10] This polypeptide is frequently used to mimic the effects of proteins on phospholipid bilayers.[1,12–14] Its advantages are its known chemical structure and its known helical conformations, its considerable stability, and its ready availability. It is believed that dimeric GA forms channels which span the hydrocarbon regions of a lipid bilayer. Chapman and co-workers have extensively studied GA in lipid dispersions with excess water by a variety of physical techniques, and their results and characterizations are important for the present study.[1,12] They find that the dimeric GA is incorporated into the lipid bilayer, and they regard it as a model for the interactions of the polypeptide segments of transmembrane proteins within the hydrocarbon regions of the lipid bilayers.

The preparation of well-aligned lipid multilayers containing GA is itself a nontrivial, yet crucial, task. We have adapted our alignment technique to this purpose, so that we are able to achieve well-aligned samples for concentrations of GA ≤4 M% (by M% we mean moles of GA per 100 mol of lipid).

We, indeed, find that the GA does induce substantial "disorder" on a submicroscopic scale, which is clearly evident below T_c, the main transition (i.e., in the gel phase). We show below that these observations are fundamentally different in a number of ways from the model of immobilized boundary lipids proposed by previous workers.[3–5,15,16] It is our belief that our clear discrimination of the heterogeneity in the bilayer induced by the GA and our determination of the molecular properties of this heterogeneity do constitute significant new results in understanding the polypeptide–GA interaction. It furthermore emphasizes the great value of combining ESR studies on well-aligned samples with careful theoretical simulations.

II. Experimental Section

The preparation and alignment of the lipid mixtures and the characterization of the macroscopic alignment of the samples are substantially the same as described in the preceding paper[10] on pure lipid samples (hereafter referred to as part 1). We describe here aspects of the procedure specifically related to samples containing gramicidin A (GA).

Lipid mixtures including nitroxide and containing different amounts of GA were prepared at the same time, together with a mixture without GA to serve as a standard. A freeze-dry method was used and care was taken to ensure that the water contents of the various lipid mixtures were equal. A typical procedure is as follows. A constant volume of benzene solution of nitroxide was added into each 2-mL glass flask with a ground joint con-
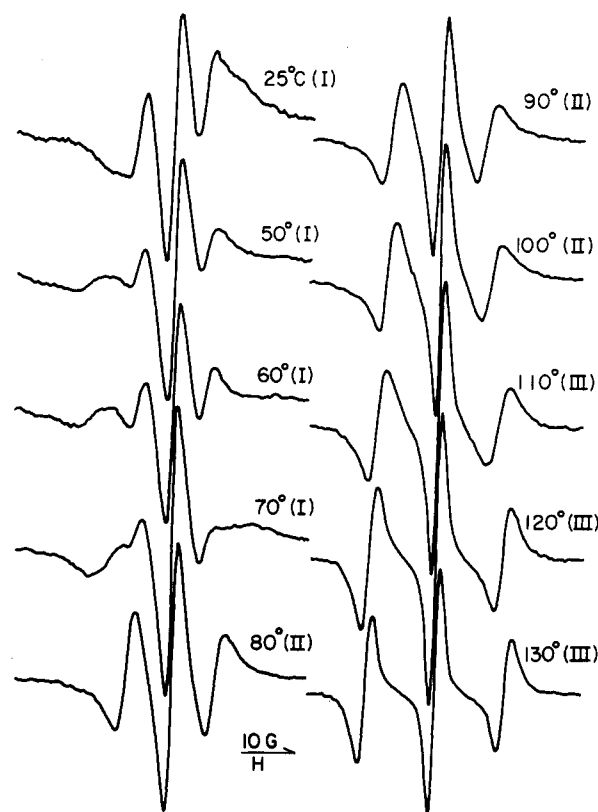

Figure 1. ESR spectra at various temperatures from CSL in DPPC hydrated to 3 wt % and containing 2 M% GA. Spectra are for $\theta = 0°$ corresponding to parallel alignment of the magnetic field and the normal to the bilayers. Phase I is the low-temperature gel phase, phase II is the main liquid crystalline phase, and phase III is a high-temperature liquid crystalline phase.

taining 25 mg of DPPC, in order to form a 0.5 M% nitroxide mixture with DPPC. Subsequently, the required volumes of a benzene–methanol solution (95:5 v/v) of GA were introduced into the flasks. The solvent in each flask was then adjusted to a constant volume (120 μL) by adding the appropriate volume of the benzene–methanol (95:5 v/v) solution. After complete dissolution of the solutes, all flasks were linked to a vacuum line and the solutions were quickly frozen with liquid N_2. The frozen solutions in a dry ice–isopropyl alcohol cold bath were evacuated for 2 days at room temperature to ensure solvent removal. The dry solids were crushed to fine powders and then were hydrated with deionized water under Ar atmosphere.

Hydrated lipid mixtures were oriented by the compression technique described in detail in part 1. The lipid mixture, sandwiched between 0.8 × 2.2 cm glass plates, was compressed repeatedly for a few minutes above the gel-to-liquid crystalline phase transition. The optimal temperature for compression depends strongly on the GA content and slightly on the water content. For aligning the DPPC samples with 0–4 M% of GA hydrated to 3 and 7 wt %, the optimal temperatures are in the range of 80–90 °C. The typical thickness of the oriented multilayers that we prepared is 10 μm (~2000 bilayers). When small amounts of fine defects remained over the sample region, then heating to 90–100 °C was effective in eliminating them. (The dispersion samples were prepared from the hydrated lipid mixtures placed directly into a cylindrical tube.)

The precise water content after the alignment procedure was determined by measuring T_c, the temperature of the main transition, using the pure lipid samples prepared at the same time as standards (cf. part 1). The aligned samples were then studied by ESR and polarizing microscopy methods as described previously.[10] Only defect-free samples (except as noted below) were used in the ESR studies. By defect-free samples we mean less than 3% defect area over the entire sample, as determined by polarizing microscopy.

(8) E. Meirovitch, D. Igner, E. Igner, G. Moro, and J. H. Freed, *J. Chem. Phys.* **77**, 3915 (1982); E. Meirovitch and J. H. Freed, *J. Phys. Chem.*, in press.

(9) L. Kar, E. Ney-Igner, and J. H. Freed, *Biophys. J.*, submitted.

(10) H. Tanaka and J. H. Freed, *J. Phys. Chem.*, in press (hereafter referred to as part 1).

(11) I. C. P. Smith and K. W. Butler, ref 5, Chapter 11.

(12) D. Chapman, B. A. Cornell, A. W. Eliasz, and A. Perry, *J. Mol. Biol.*, **113**, 517 (1977).

(13) E. Oldfield et al., *Proc. Natl. Acad. Sci. U.S.A.* **75**, 4657 (1978); S. Y. Kang et al., *Biochemistry*, **18**, 3257 (1979); S. Y. Kang, H. S. Gutowsky, and E. Oldfield, *ibid.*, **18**, 3268 (1979).

(14) J. H. Davis, R. S. Hodges, and M. Bloom, *Biophys. J.* **37**, 170 (1982); J. H. Davis, D. M. Clare, R. S. Hodges, and M. Bloom, *Biochemistry*, **22**, 5298 (1983).

(15) P. C. Jost, O. H. Griffith, R. A. Capaldi, and G. Vanderkooi, *Proc. Natl. Acad. Sci. U.S.A.*, **70**, 480 (1973).

(16) P. F. Knowles, A. Watts, and D. Marsh, *Biochemistry*, **18**, 4480 (1979).

III. Results and Discussion

A. Temperature Dependence of the ESR Spectra. Figure 1 shows the ESR spectra of CSL in oriented DPPC multilayer with 3% water by weight containing 2 M% GA, over the temperature range of 25–130 °C. It includes spectra from phase I, which is the gel phase, phase II, the primary L_α or liquid crystalline phase, and phase III, a high-temperature liquid crystalline phase characterized by low ordering.[10] All spectra are for the normal to the plates aligned parallel to H_0, the magnetic field (i.e., $\theta = 0°$). In these samples the extent of the main transition (I–II transition) and that of the II–III transition lie between 70 and 80 °C between 100 and 110 °C, respectively. We first observed the latter phase transition with pure DPPC and DMPC samples and described the character of the transition and of phase III in the preceding paper.[10] The respective transition temperatures (T_{I-II} and T_{II-III}) are almost equivalent to those in the corresponding pure DPPC samples. This correspondence of the transition temperatures was observed for the range of [GA] from 0 to 4 M% in the present study.

The most remarkable feature of the effect of GA, which can be noticed from Figure 1, is that the presence of GA induces a heterogeneity in the lipid multilayer. The heterogeneity is clearly observed as a "two-component" type of ESR spectrum in phase I, the gel phase. The effect of GA on the spectrum from phases II and III is less dramatic, appearing as a broadening of the outer two lines, with this effect more pronounced for phase II. We analyze these features later by spectral analysis.

Figure 2, A and B, shows the ESR spectra of CSL in well-aligned DPPC samples hydrated to 7 wt % with no GA and with 2 M% GA. From a comparison of the spectra of both samples, it can be found that the heterogeneity effect of GA on lipids is conserved at 7 wt % water, although the main transition range is lowered to between 60 and 70 °C. A similar temperature dependence of the ESR spectra is observed with 16PC, as represented by the spectra of the pure DPPC and 2 M% GA–DPPC samples hydrated to 7% (cf. Figure 3, A and B). In these figures the two components of the ESR spectra in phase I collapse to a single component in phase II with a value for the splitting lying between those for the two components in phase I. In the case of 16PC, the effect of GA on the spectral features in phase II is very small (because of the small ordering at the labeled position as will be shown later).

As described above, the features observed in the ESR spectra that are caused by the presence of GA depend strongly on the temperature (and phase). They are most pronounced in phase I and minimal in phase III. We can use the results on CSL and 16PC to describe the effects of GA on the main chain region (i.e., roughly the first 10 C atoms which are highly ordered[2]) and the terminal portion, because CSL and 16PC report on the main part and terminal portion of the chain, respectively (cf., ref 1).

The concept of "heterogeneity" is important for understanding the effect of GA (and possibly other polypeptides and proteins) on lipids. An aim of this study is to clarify the details of this heterogeneity, which is clearly seen in the phase I spectra. Some membrane researchers accept the idea that the presence of polypeptide (or protein) makes membrane systems heterogeneous. However, this concept should be understood in relation to the conditions of temperature and water content. Under some conditions our results indicate that membrane systems can appear to be homogeneous in spite of the presence of polypeptides. In fact, as we already observed, the multilayers appear to be homogeneous in the liquid crystalline phases: II and III.

B. Heterogeneities Caused by GA vs. Those Caused by Defects. Oriented multilayer samples can be heterogeneous not only because of the presence of GA but also because of the presence of defects. To discriminate the intrinsic effect of GA from the effects of defects, we used polarizing microscopy to observe the morphology and transmitted photointensity of oriented samples under crossed polarizers. In the preceding paper on pure lipid samples, we demonstrated that the quality of lipid alignment can be determined by such observations. This is based on our finding that the optical observations of defects (type and "quantity") correspond well with
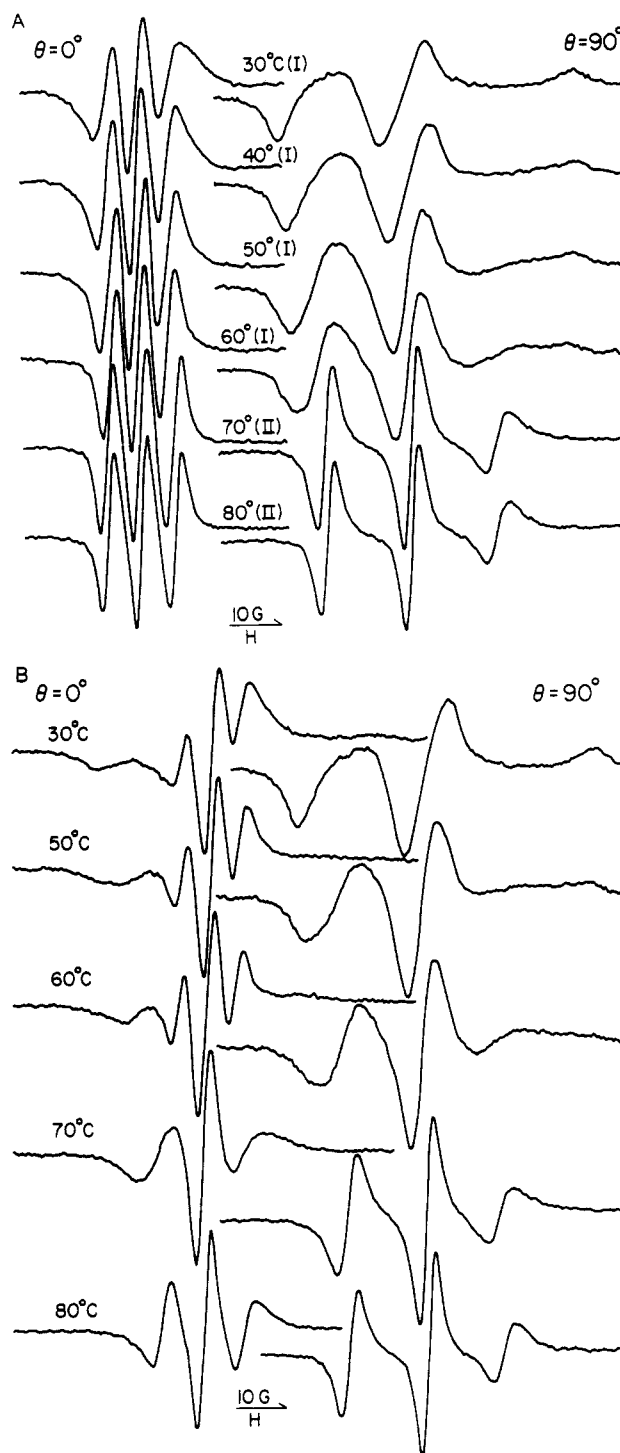

Figure 2. ESR spectra at various temperatures from CSL in DPPC hydrated to 7 wt %: (A) 0 M% GA; (B) 2 M% GA. Spectra are shown for $\theta = 0°$ and 90° orientations.

the ESR observations of their effects. In particular, "black membranes", having no appreciable defects (<3%) as detected optically, produce ESR spectra with the highest ordering estimated simply from line splittings. The same optical criteria on the quality of sample alignment was also used for GA-containing samples. The defect-free samples containing GA that were used in the present study were equivalent to the corresponding pure lipid samples in their morphology and transmitted photointensity under crossed polarizers, at least, as far as measured within the sensitivity of the photodetector used in the present study.

We observed the same types of defects for GA-containing samples as those for pure lipid samples. Especially, type a defect, consisting of regions of unoriented materials, was most important because of its frequency of occurrence and its extent. This is
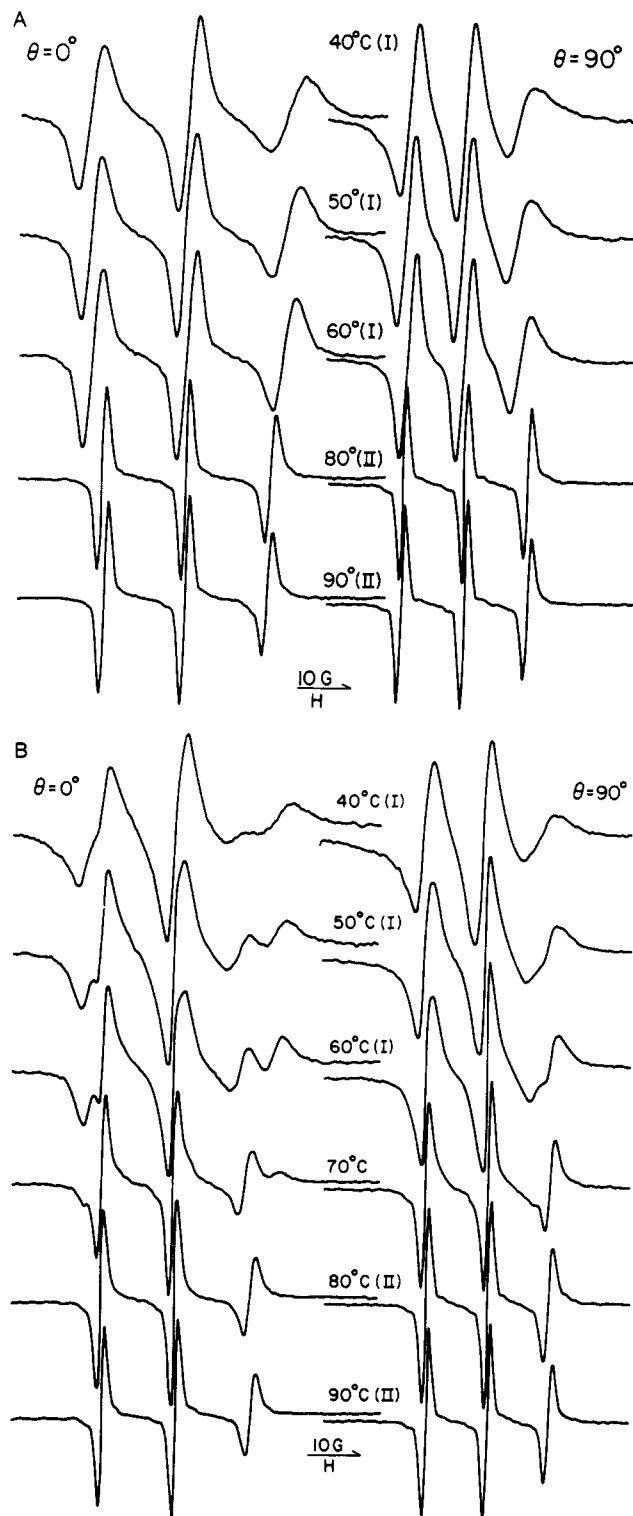
Figure 3. ESR spectra at various temperatures from 16PC in DPPC hydrated to 3 wt %: (A) 0 M% GA; (B) 2 M% GA. Spectra are shown for $\theta = 0°$ and 90° orientations.

Figure 4. ESR spectra at 50 °C (phase I) and at 90 °C (phase II) from 16PC in DPPC hydrated to 3 wt % and containing 0.5 M% GA. Spectra are for $\theta = 0°$. At each temmperature a shows the spectrum from a defect-free sample, while b shows the spectrum from a sample with 50% of its area unoriented (i.e., type a defect). Dashed lines show simulation.

because the presence of GA will naturally tend to promote macroscopic defects. Nevertheless, our techniques of alignment still allowed us to align samples containing as much as 4 M% GA and to achieve our defect-free criterion. Clearly, it is important for us to distinguish submicroscopic "heterogeneity" due to the GA from the heterogeneity due to macroscopic defects. While our primary criterion was polarizing microscopy as already described, we compare in Figure 4 the ESR spectra of 16PC in 3% water–DPPC in phase I containing no defects with those from a sample with 50% by area of type a defect. Both samples contain 0.5 M% GA. While at 50 °C the spectra for the two cases are similar, that from the defect-free sample shows greater resolution in the
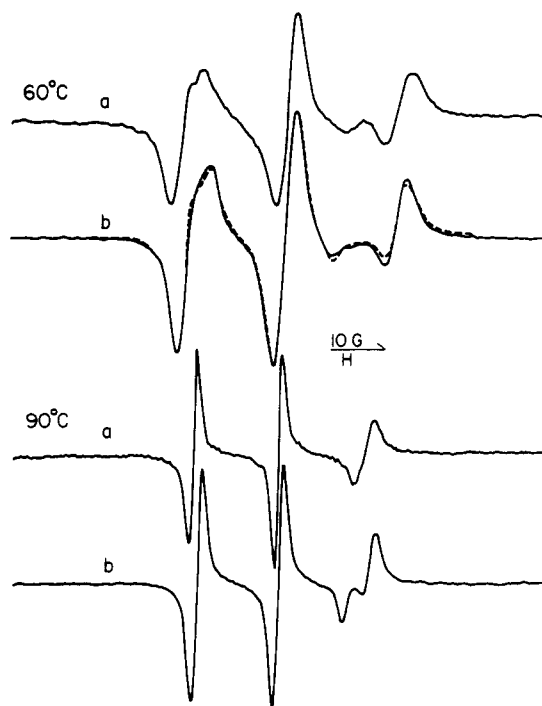
low- and high-field peak regions, especially in the details pertaining to the inner (or disordered) component. However, at 90 °C (phase II), the defect-free sample is the single-component type, in contrast to the two-component pattern for the defect-containing sample. Thus, from the point of view of ESR spectral features, effects of GA vs. those from macroscopic defects could be clearly distinguished in phase II, while more subtle but significant differences exist in phase I. (In part 1, we did show that the two components in the spectra from defect-containing samples could be respectively assigned to sample regions with defects and well-aligned regions.)

One might suppose that the two-component type of spectra observed with optically defect-free samples in phase I could be ascribed to the presence of very fine defects that are unresolved optically. The resolution of our microscope corresponds to ca. 1 μm (i.e., about 200 bilayer thickness on the molecular level). However, a large number of fine defects somewhat smaller than this resolution do still affect the transmitted photointensities measured between crossed polarizers, because samples containing such defects appear pale black or gray but not fully black. Indeed, we often observed such a phenomenon when the polygonal-array defects (defect type b, cf. part 1) first form at T_c, the main transition temperature. These first form as individual fine polygons which are unresolved morphologically, but they do change the optical transmittance as well as the ESR spectral features (cf. below). (In time these defects become large enough to be observed morphologically).

From these considerations we are able to conclude that the spectral features illustrated in Figures 1–3 are intrinsic to oriented lipid samples containing GA and that they reflect the nature of the lipid–GA interaction which, in terms of optical resolution, is characterized by no (or at most a very small) change of optical transmittance of the sample compared to GA-free samples. (It is difficult for us to estimate the smallest size of defect that, if extensive, would affect the optical transmittance. A reasonable lower bound might be 10% of the resolution, or about 0.1μm.)

Figure 5 shows another effect of defects on the ESR spectra, observed with samples of CSL in 1 M% GA–DPPC at 7 wt % water containing 20% area of type a defects (i.e., unoriented materials). As seen in this figure, the spectra of the defect-containing sample are quite different in appearance from those
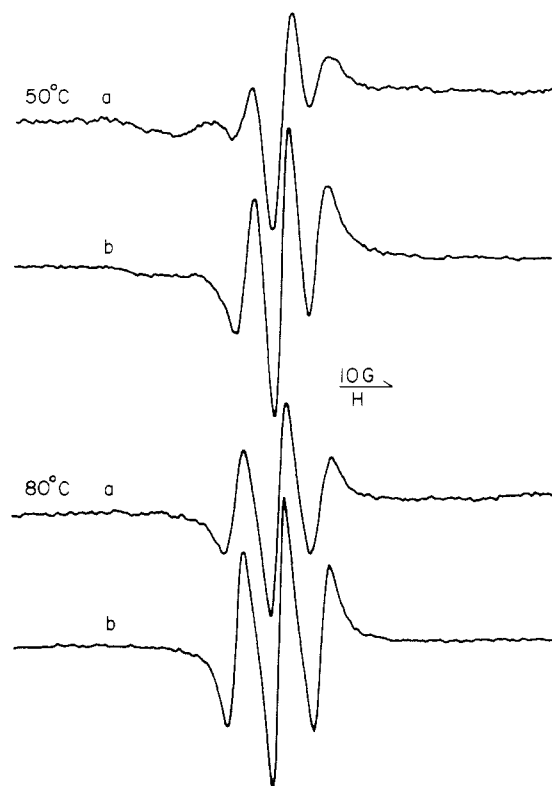
Figure 5. ESR spectra at 50 °C (phase I) and at 80 °C (phase II) from CSL in DPPC hydrated to 3 wt % and containing 1 M% GA. Spectra are for $\theta = 0°$. At each temperature a shows the spectrum from a defect-free sample, while b shows the spectrum from a sample with 20% of its area unoriented (i.e., type a defect).

from defect-free samples. In fact, by comparing them with spectra in part 1 from pure lipids containing no GA, we find they are closer to the latter! We believe that this can be explained in terms of phase separation; i.e., the unaligned or defect regions act as a different phase from the aligned regions, which then become rich in GA, while the aligned regions become GA deficient. Such a phase separation, which was observed optically by Powers,[17a] may occur in the alignment process at higher temperatures. The GA-rich regions produce a significantly broadened component that therefore appears to be weak, and may be found outside the sharper component. Similar spectra were obtained with oriented samples which were prepared from a lipid–GA mixture in which the solvent (benzene–methanol 95/5 v/v) was slowly evaporated from the liquid solution. In this case, GA was not mixed thoroughly with lipid because of their different solubilities, resulting in a phase separation of GA and lipid. We believe that this observation confirms the above inferences on the role of phase separation of GA. In fact, we find that the presence of defects, even if the defect area is as low as 20%, will noticeably influence the ESR spectral features of the gramicidin-containing samples.[17b]

We find that polygonal array (type b) defects which appear just above T_c produce a two-component spectral feature similar to that of the corresponding pure lipid sample containing the same type of defect. Thus, in the case of this defect, spectra of the oriented samples both with type b defects and without any defects can easily be discriminated.

In summary then, we find that it is possible to distinguish between the effects of the macroscopic defects and the submi-
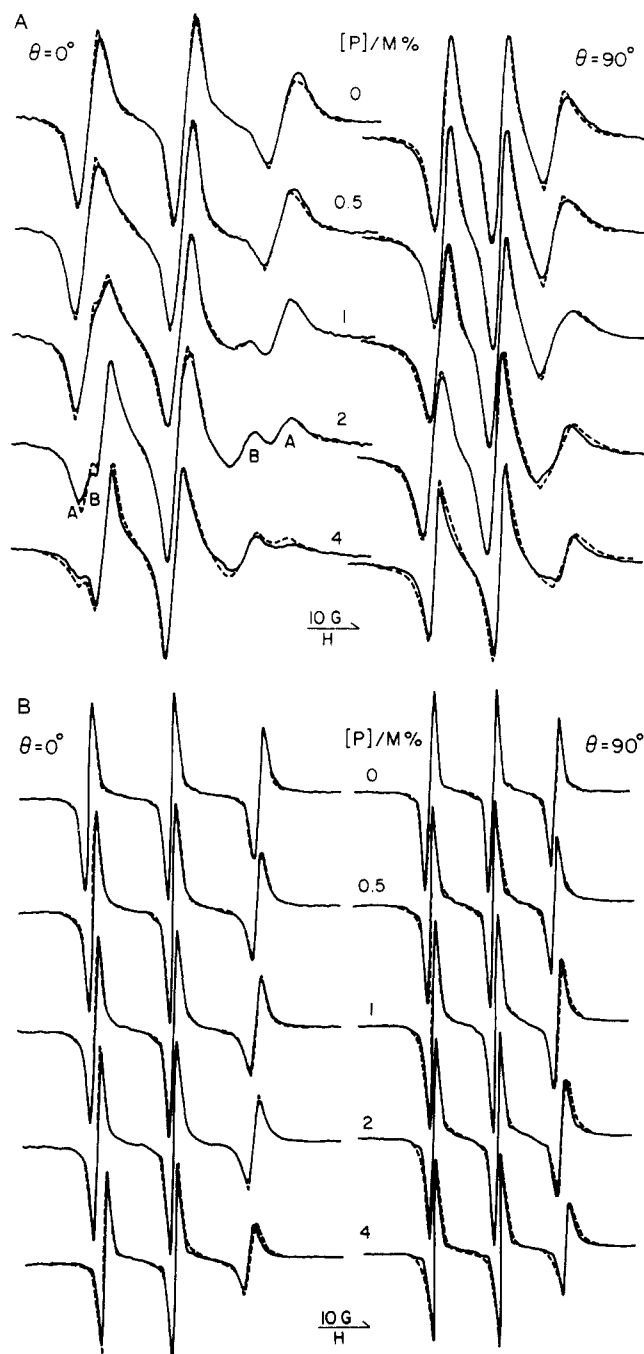
(17) (a) L. Powers and P. S. Pershean, *Biophys. J.*, **20**, 137 (1977); L. Powers, Ph.D. Thesis, Harvard University, Cambridge, MA, 1977. (b) We are able to prepare samples of 20M% GA and 3–7 wt % H₂O, but much higher annealing temperatures of ca. 140 °C were required before the compression technique would lead to alignment. The best samples, however, had ca. 10% defects. The ESR spectra exhibit no significant angular dependence. Instead they have an appearance corresponding to the disordered lipids in the gel phase up to temperatures much higher than the T_c for the pure lipid samples, and no clear phase transition is observed from them.

Figure 6. ESR spectra from 16PC in DPPC hydrated to 7 wt % for concentrations of GA ranging from 0 to 4 M%. Spectra are shown for $\theta = 0°$ and 90°: (A) 50 °C corresponding to phase I; (B) 80 °C corresponding to phase II. Dashed spectra are simulations based on Tables I and II, respectively. In Figure 6A, the ordered and disordered components are labeled A and B, respectively.

croscopic effects of added GA reasonably to conclude that the "heterogeneity" in the ESR spectra that is caused by GA originates from structural changes on the lipid organization through lipid–GA interaction at the molecular level.

C. Dependence of the ESR Spectra on GA Concentration. Figure 6, A and B, shows the ESR spectra of 16PC in 7 wt % water–DPPC oriented multibilayers free from defects ($\leq 3\%$ of area), containing various concentrations of GA and for phase I and phase II, respectively. As seen in Figure 6A, introduction of GA into the multibilayers leads to the development of a new spectral component which is distinct from the original component. The original component remains nearly the same as the spectrum of the corresponding pure lipid sample with respect to the positions of its peaks. One sees, from a comparison of the $\theta = 0°$ and 90° spectra, that the new component is characterized by very small

A
$\theta = 0°$ [P]/M% $\theta = 90°$

Figure 8. Graphs of measured separation between low-field and middle spectral lines (i.e., "apparent" splitting) vs. [P], the concentration of GA in M% for samples of CSL and 16PC in DPPC hydrated to 7 wt % at 80 °C (phase II). The closed and open circles are for CSL, $\theta = 0°$ and 90°, respectively; the closed and open squares are for 16PC, $\theta = 0°$ and 90°, respectively.
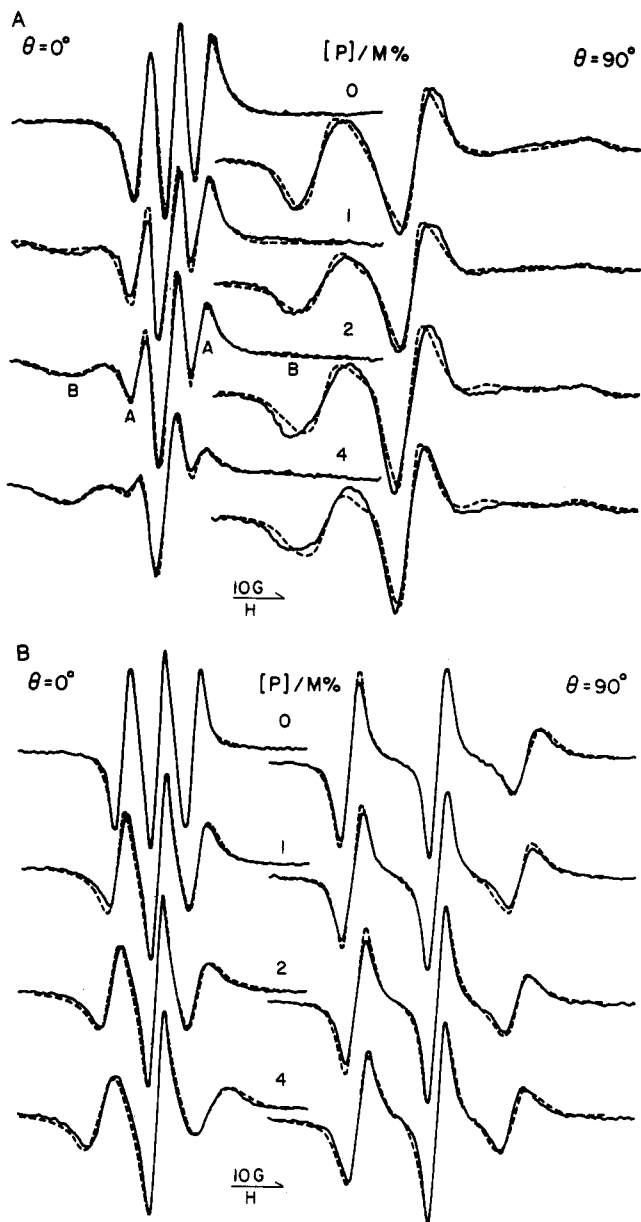

Figure 7. ESR spectra from CSL in DPPC hydrated to 7 wt % for concentrations of GA ranging from 0 to 4 M%. Spectra are shown for $\theta = 0°$ and 90°: (A) 50 °C corresponding to phase I; (B) 80 °C corresponding to phase II. Dashed spectra are simulations based on Tables I and II, respectively. In Figure 7A, the ordered and disordered components are labeled A and B, respectively.

ordering, since there is not a large change in the apparent splittings at $\theta = 0°$ and 90°. It is also shown in the figure that with increase of [P] (i.e., the concentration of GA in M%) the new component (which we shall refer to as the disordered component) increases in intensity, relative to that of the original or ordered component. On the other hand, in the liquid crystalline phase shown in Figure 6B, a single-component type of spectrum persists even as [P] increases. The primary change is a decreasing high-field peak height relative to the central peak (i.e., h_1/h_0 decreases as [P] increases).

These same trends are also found for the CSL spectra. The ESR spectra of CSL in 7% water–DPPC as a function of [P] are shown in Figure 7. The apparent splittings measured from the 80 °C spectra are plotted vs. [P] in Figure 8. We observe in this figure that the orderings of 16PC and CSL both decrease monotonically with [P] (and this is confirmed below by detailed simulations). We show in Figure 9 spectra for CSL in the high-temperature liquid crystalline phase (phase III) at 120 °C for 3 wt % water. Here we see sharp and well-resolved lines. The apparent splittings obtained from Figure 9 are plotted as a function
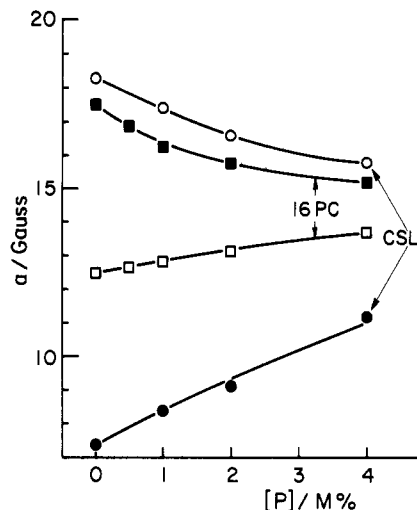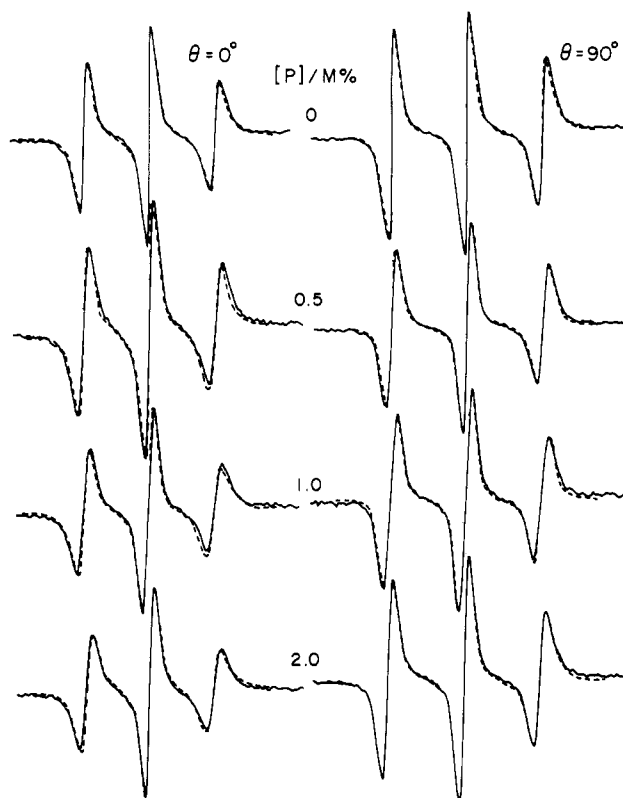

Figure 9. ESR spectra at 120 °C (phase III) from CSL in DPPC hydrated to 3 wt % for concentrations of GA ranging from 0 to 2 M%. Spectra are shown for $\theta = 0°$ and 90°. Dashed spectra are simulations based on Table III.

of [P] in Figure 10 and are compared with those for 3% water–DPPC samples obtained at 80 °C (phase II). The [P] dependence at 80 °C is similar to that for the corresponding CSL sample hydrated to 7 wt % shown in Figure 8, but the difference between the splittings at $\theta = 0°$ and 90° for the 3 wt % sample is slightly increased at each respective [P], indicating an increased ordering for the sample with lower water content. However, at 120 °C, the ordering as inferred from the splitting (cf. Figure 10) first decreases and then increases with increase of [P], with a minimum at ~0.5 M%. Thus, the effect of GA on the ordering is different in the two liquid crystalline phases.

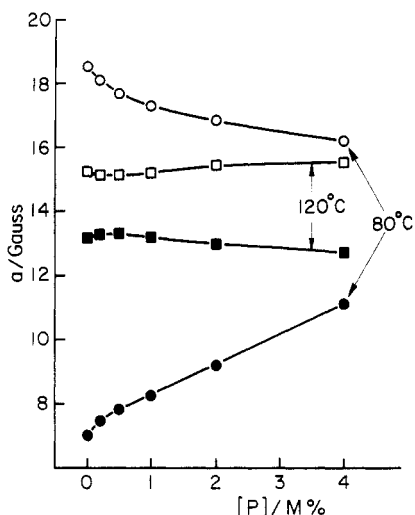*D. Dependence of the ESR Spectra on* [H₂O]. One finds from

Figure 10. Graphs of measured separation between low-field and middle spectral lines (i.e., "apparent" splitting) vs. [P], the concentration of GA in M% for samples of CSL in DPPC hydrated to 3 wt %. The closed and open circles are for 80 °C (phase II), $\theta = 0°$ and 90°, respectively; the closed and open squares are for 120 °C (phase III), $\theta = 0°$ and 90°, respectively.
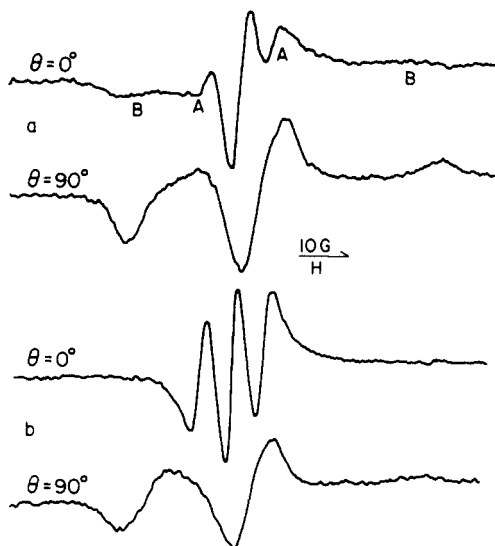

Figure 11. ESR spectra at 30 °C (phase I) from CSL and DPPC containing 4 M% GA and hydrated at (a) 7 and (b) 17 wt %. Spectra are shown for $\theta = 0°$ and 90°.

an examination of Figures 1, 2, and 11 that for both 16PC and CSL the signal intensity of the disordered component decreases with increase of water content in this range. In figure 11 we show the ESR spectra of CSL in oriented DPPC hydrated to 7% and 17% (±5%), obtained at 30 °C. [Hydration to 17 wt % was achieved by applying a humidity technique[17] to a 7 wt % sample. Such samples show more optical defects (≤10%)]. The disordered component, which is prominent at 7 wt % water, has disappeared in the spectra of the 17 wt % water sample. On the basis of the above results, it can be said that the existence and the extent of the disordered component is sensitive to water content such that its signal intensity decreases with increase of the amount of water incorporated between the bilayers.

E. Simulations of the ESR Spectra. Quantifying the Role of GA. The ESR spectra shown in Figures 6, 7, and 9 were analyzed in quantitative detail by utilizing our theoretical methods of spectral analysis.[8] This analysis[8] yields the ordering of the labels, as well as its asymmetry, and it also yields the rate of rotational reorientation and its anisotropy. The rotational rate is a measure of the fluidity in the mean potential of the surrounding molecules which determines the ordering. Our objectives are to study the influence of GA concentration on lipid organization (both

its structure and motion) at typical temperatures in each ordered phase (i.e., phases I–III).

As already described, the ESR spectra in phase I, the gel phase, consist of two components of which the disordered component increases in signal intensity, relative to the ordered component, with increase in [P]. This is reasonably interpreted on the basis of the idea that "disordered lipids", responsible for the disordered component, are created around the polypeptide molecule. The disordered (or boundary) lipids may be considered from two points of view. That is, either these lipids are disordered on a submicroscopic (or molecular) level, or else they retain their ordering on a molecular level, but the principal direction of this ordering becomes nearly randomized by the presence of GA. In the former model, lipids which are disordered at the molecular level experience a large reduction in their ordering parameter $S \equiv \langle D_{00}^2 \rangle$ (we shall refer to this as molecular disorder). In the latter model, the "disordered" lipids still possess large molecular ordering parameters, comparable to that of the respective ordered phase in the absence of GA, but they are disordered in their preferred direction of alignment (i.e., the director) by the presence of the GA (this is referred to below as director disorder). These two models are clearly to be regarded as limiting ones. It seems reasonable to allow for the possibility that the molecular diffusion ($R_\perp$ and $R_\parallel$) of the boundary lipids is affected by the lipid–GA interaction. Furthermore, although the boundary lipids are most dramatically affected by the presence of GA, as evidenced by the ESR spectrum, a more long-range but significantly weaker effect on the remaining well-aligned (or bulk) lipids might be expected. This latter notion is supported by spectral substractions utilizing ESR spectra of oriented DPPC samples with and without GA that are hydrated to the same water content and are at the same temperature. However, perfect substracted spectra were never obtained, indicating a small difference between the spectra from the pure lipids and from the bulk lipids in the presence of GA. Last of all, we may expect that the large effects on boundary lipids and small effects on bulk lipids may themselves be functions of distance from the GA molecules, but we have not sufficient spectral resolution to discern such subtleties. We assumed a two-site model of boundary and bulk lipids which take different molecular orderings.

In summary then, we wish, by spectral simulations, to analyze the ESR spectra in terms of boundary and bulk lipids each with its distinctive properties. Given that this is a very large task, and the spectral resolution, while good, is still a constraint, we took the simplest model for our simulations. That is, we used a two-site model consisting of boundary and bulk lipids, where the boundary lipids are described in terms of "molecular disorder" (cf. above discussion). The concept of "director disorder" will be further discussed in subsection G, although we did not perform the more sophisticated spectral simulations required for this model in the present work. Thus, we analyzed the spectra from phase I in terms of the ordering and motional properties of two types of lipid, with a single set of ordering and motional parameters for each type. We assumed that as [P] increased, the dominant effect was the increase of boundary to bulk lipid, and we only made small adjustments to the properties of the bulk lipids.

The results analyzed on the basis of a simple two-site, molecular disorder model are shown in Table I. Here the ordering and diffusion parameters of the boundary and bulk lipids are listed together with their signal intensities (defined as mole fractions: C_O and C_D for the ordered and disordered lipids, respectively) of their spectral components. In this analysis, trial values of N, the rotational anisotropy parameter, were used that are consistent with the previously found correlation between N and $\langle D_{00}^2 \rangle$ spin-labels in pure DPPC (cf. parts 1). We used the more resolved 16PC spectra to estimate the mole fractions C_O and C_D, and then we utilized the same values in simulating the CSL spectra. We show in Figures 6A and 7A the comparison between the experimental spectra and the spectra simulated with the parameters of Table I. The fits are seen to be quite good, although not perfect.

It is clear from Table I that the boundary and bulk lipids are quite similar in their respective diffusion constants (especially in

TABLE I: Parameters for Molecular Ordering and Anisotropic Rotation of 16PC and CSL in DPPC Hydrated to 7 wt % at 50 °C (Phase I), Including Ordered vs. Disordered Components Due to Presence of GA[a]

compont	$\langle D_{00}^2\rangle$	$\langle D_{02}^2 + D_{0-2}^2\rangle$	$R_\perp/s^{-1}$	$R_\parallel{}^c/s^{-1}$	N	$T_2^{*-1}/$ G
		16PC				
pure	0.32	−0.11	1.9×10^8	3.8×10^8	2	1.4
ordered	0.30	−0.12	1.8×10^8	3.6×10^8	2	1.4
disordered	0.03	0	1.8×10^8	2.2×10^8	1.2	1.4
		CSL				
pure	0.88	−0.005	5.0×10^5	7.5×10^7	150	1.5
ordered	0.90	−0.008	5.0×10^5	7.5×10^7	150	1.7
disordered	0.13	0	4.0×10^6	6.4×10^7	16[e]	1.7

[GA]/M%	0	0.5	1.0	2.0	4.0
$P:L^f$		1:200	1:100	1:50	1:25
$100C_O{}^b$	100	86	60	35	13
$100C_D{}^c$	0	14	40	65[d]	87
no. of disordered lipids per GA dimer	0	56	80	65	44

[a] Estimated errors: ±5% in $\langle D_{00}^2\rangle$, ±30% in $\langle D_{02}^2 + D_{0-2}^2\rangle$, ±10% in $R_\perp$, and ±30% in N. [b] Mole fraction of ordered lipid. [c] Mole fraction of disordered lipid. [d] From preliminary simulations of 3 wt % samples, C_D is increased to about 80%. [e] An $N = 16$ was used for the disordered component to better simulate the large broadening of the $M = \pm1$ lines. [f] Ratio of component percentages.
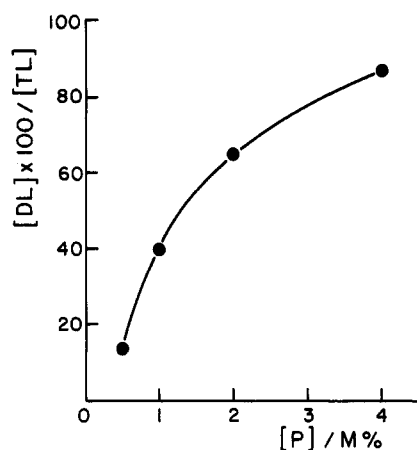

Figure 12. Graph of percent of disordered lipid (i.e., 100[DL]/[TL]) vs. concentration of GA, [P] in M% based on Table I for 50 °C (phase I) and hdyrated to 7 wt %.

TABLE II: Parameters for Molecular Ordering and Anisotropic Rotation of 16PC and CSL in DPPC Hydrated to 7 wt % at 80 °C (Phase II) as a Function of GA Concentration[a]

$[P]^b$	$\langle D_{00}^2\rangle$	$\langle D_{02}^2 + D_{0-2}^2\rangle$	$R_\perp/s^{-1}$	$R_\parallel/s^{-1}$	N	$T_2^{*-1}/$G
		16PC				
0	0.17	0	1.0×10^9	1.2×10^9	1.2	
0.5	0.15	0	8.1×10^8	9.7×10^8	1.2	
1.0	0.13	0	6.8×10^8	8.2×10^8	1.2	0.8
2.0	0.095	0	5.0×10^8	6.0×10^8	1.2	
4.0	0.073	0	4.3×10^8	5.2×10^8	1.2	
		CSL				
0	0.74	−0.01	1.2×10^7	6.0×10^8	50	
1.0	0.53	0	2.9×10^7	4.6×10^8	16	
2.0	0.42	0	2.7×10^7	4.3×10^8	16	1.2
4.0	0.24	0	2.5×10^7	4.0×10^8	16	

[a] Estimated errors: ±5% in $\langle D_{00}^2\rangle$, ±30% in $\langle D_{02}^2 + D_{0-2}^2\rangle$, ±10% in $R_\perp$, and ±20% in N. [b] [P] is GA concentration in M%.

TABLE III: Parameters for Molecular Ordering and Anisotropic Rotation of CSL in DPPC Hydrated to 3 wt % at 120 °C (Phase III) as a Function of GA Concentration[a]

$[P]^b$	$\langle D_{00}^2\rangle$	$\langle D_{02}^2 + D_{0-2}^2\rangle$	$10^{-8}R_\perp/$ s^{-1}	$10^{-9}R_\parallel/$ s^{-1}	N	$T_2^{*-1}/$G
0	0.206	0.057	1.5	2.4	16	
0.5	0.175	0.045	1.2	1.9	16	
1.0	0.200	0.058	1.1	1.8	16	1.0
2.0	0.267	0.068	1.0	1.6	16	
4.0	0.318	0.081	0.9	1.4	16	

[a] Estimated errors: ±2% in $\langle D_{00}^2\rangle$, ±30% in $\langle D_{00}^2 + D_{0-2}^2\rangle$, ±10% in $R_\perp$, ±20% in N, and ±0.2 G in T_2^{*-1}. [b] [P] is GA concentration in M%.

distinctly different types of lipid or because exchange between bulk and boundary lipid regions has become too fast. We therefore analyzed our results in terms of a single (possibly an average) site, and we again adjusted N in accordance with the previously observed relation between N and $\langle D_{00}^2\rangle$ (cf. ref 1). In Table II we give the ordering parameters and rotational diffusion coefficients for 16PC and CSL obtained for phase II (80 °C) from 7% water–DPPC samples. These results show a monotonic reduction of the diffusion rate, primarily monitored by $R_\parallel$, with increase of [P], together with a decrease of the ordering $\langle D_{00}^2\rangle$. The good agreement between experimental and simulated spectra utilizing the parameters of Table II is illustrated in Figures 6B and 7B.

The spectra in the high-temperature liquid crystalline phase, phase III, were analyzed in the same manner as those for phase II. The results obtained for CSL in DPPC with 3 wt % water at 120 °C are given in Table III. Again we find that the diffusional rates decrease with increase of [P]. However, in this phase the ordering is found to increase as [P] increases (for [P] > 0.5 M%) in sharp contrast to phase II, but confirming our preliminary analysis in subsection C. The good fits between experiment and simulations based upon the parameters of Table III are illustrated in Figure 9.

F. Lipid–GA Interaction. We have seen that the presence of GA leads to effects on lipid organization, molecular ordering and rotational diffusion and these effects are different in detail in each phase (I–III). We believe that these various effects can be explained as the consequence of two competing features of the lipid–GA interaction:

(1) The presence of GA molecules induces a disordering of the lipids in their vicinity, either by molecular disorder and/or by director disorder. We refer to this as the disordering feature.

(2) The presence of GA molecules hardens the membrane systems, i.e., makes them more solidlike. This tendency is exemplified by reduced fluidity (i.e., a reduction in the rotational diffusion coefficients) and by increasing the order. This is the hardening feature.

Clearly the disordering effect of boundary lipids due to molecular disorder and the hardening of overall order are conflicting. However, if director disorder is invoked, then it does not necessarily

$R_\perp$), although very different in their ordering $\langle D_{00}^2\rangle$. Another feature one notes from this table is that the number of boundary lipids per GA molecule does not remain constant vs. [P]. This is emphasized in the nonlinear plot of C_D ($\equiv 100[DL]/[TL]$ where [DL] and [TL] are the concentrations of disordered and total lipid) with [P] in Figure 12. This effect could most likely be a saturation effect; i.e., as $C_D > 50\%$, further addition of GA will be into lipid regions that are already at least partially disordered. In fact, for 4 M% GA, 87% of lipid molecules are of the disordered type in phase I.

We have also simulated spectra at 40 and 60 °C shown in Figures 1–3. These spectra show a variation in $\langle D_{00}^2\rangle$, $R_\perp$ and N with [P] that is similar to the results in Table I for 50 °C. Most interesting is the finding that C_D is independent of temperature in this temperature range in phase I. This temperature independence should probably be compared with the temperature independence of $\langle D_{00}^2\rangle$ observed for the gel phase.[10] Both features would then be characteristic of the "structure" of the gel phase; i.e., they are crystalline-like properties.

As discussed above, the spectra in the liquid crystalline phases are of the single-component type. That is, within the ESR time scale (ca. 7×10^{-9} s, cf. Figure 6A), one cannot distinguish ordered from disordered lipids either because there are no longer two

conflict with an overall hardening effect (cf. section IV).

In order to explain our observations in terms of these two competing features we have to further assume that feature 1 is dominant under conditions of low fluidity, while feature 2 is dominant when there is high fluidity. For the samples containing 3 and 7 wt % water that we mainly investigated in this study, the gel phase (phase I) is controlled by feature 1, while phase III is mainly controlled by feature 2. An increase in water content increases the fluidity, and this leads to the predominance of feature 2. As the amount of water is increased in phase I, there is an increase in the surface area per lipid molecule. This reduces the "disordering potential" of the GA molecule as it may be more effectively incorporated into the known hexagonal lattice.[18] This then leads to a decrease in the mole fraction of boundary lipids in phase I with an increase of water content, as shown in Figures 1, 2, and 11. With a decrease in importance of (1) the disordering feature, then (2) the hardening feature of GA should exert a more prominent role. We shall have occasion to invoke this point of view in the next subsection.

G. Comparison of Results from Oriented Samples and from Dispersions. Higher GA and Water Contents. In part 1 we compared the unoriented ESR spectra obtained from a sample of 16PC in pure DPPC (7 wt % water) contained in a cylindrical tube with simulations. (We shall refer to such unoriented samples as dispersions.) The simulations of the spectra from dispersions were based on the parameters obtained from analysis of the oriented samples, and they were produced by integrating simulations of oriented spectra for all tilt angles θ equally weighted on the unit sphere. We found good, but not perfect fits, with some discrepancy in the low-field line for phase II. We show in Figure 13, A and B, ESR spectra from dispersions for 16PC in DPPC (7 wt % water) for different amounts of GA ranging in concentration from 0 to 10 M%. Figure 13A is for spectra at 50 °C (phase I), and these results are compared with simulations based on the two-site parameters in Table I for [P] ranging from 0 to 4 M%. Similarly, Figure 13B is for 80 °C (phase II) with simulations based on the one-site parameters in Table II. In both cases the simulations are good but not perfect (the low-field discrepancy may again be seen in Figure 13B for the lower [P]). This appears to be reasonable confirmation of our model parameters and fits.

In Figure 13A we have marked the separation between the two outer peak components, a feature that is well reproduced by our simulations. We find that this peak separation is a convenient measure of ordering. In the past the McConnell S parameter has frequently been utilized to estimate ordering.[3-5] However, it has been shown by careful analysis that, in general, there can be many problems with such simple methods, largely due to effects of motion on the spectrum.[19] We have confirmed in our present simulations that, for our 16PC–DPPC spectra where $R \equiv (R_\perp R_\parallel)^{1/2} > 5 \times 10^7 \text{ s}^{-1}$, this separation d is a qualitatively useful index of ordering. We find this parameter useful in gleaning information from dispersion spectra where [P] > 4 M%, for which we do not have good quantitative parameters available from analysis of well-oriented spectra.

In Figure 13A we see that the increase of disordered component with increase in [P] that was clearly seen in the well-aligned spectra (cf. Figure 6A) now appears in both experiment and simulation as a gradual loss in the outer high-field component with increasing [P] in the dispersion. (This is, of course, not as informative as the oriented spectra. In fact, a naive analysis of Figure 13A might have led us to suppose that there were two species for 0 M% GA and one of those species disappears as GA is added!) In Figure 13B we can follow the decrease in d as [P] is increased, consistent with the results of Table II that the ordering decreases in phase II. Our observations with 10 wt % samples are also consistent with this trend.
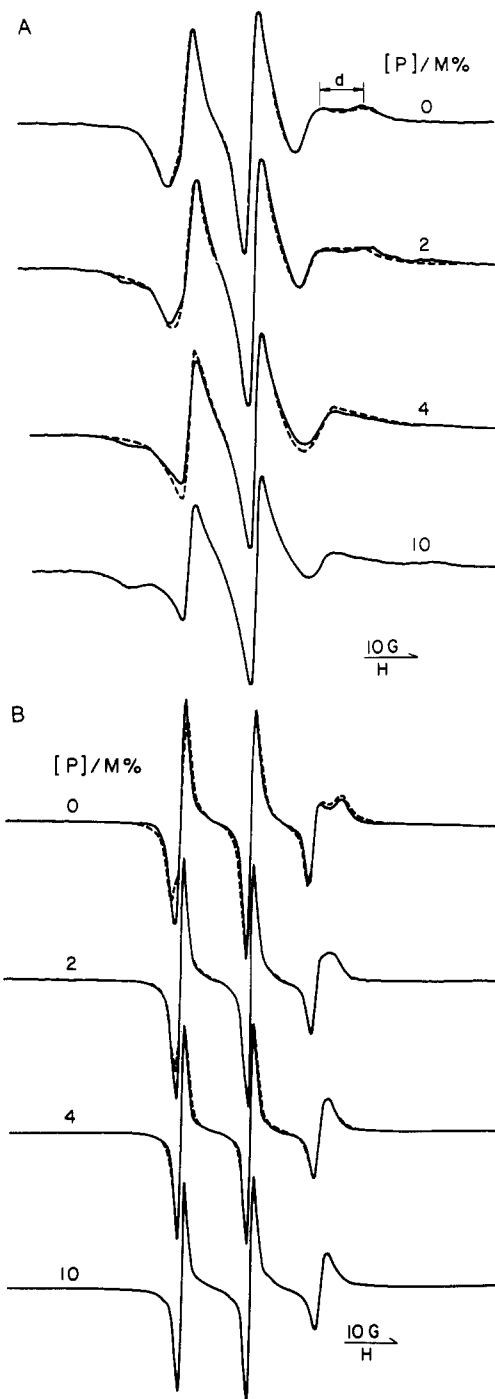
(18) A. Tardieu, V. Luzzati, and F. C. Reman, *J. Mol. Biol.*, **75**, 711 (1973).

(19) R. P. Mason, C. F. Polnaszek, and J. H. Freed, *J. Phys. Chem.* **78**, 1324 (1974); J. H. Freed in ref 5, Chapter 3.

Figure 13. ESR spectra for 16PC in unoriented DPPC dispersions hydrated to 7% for concentrations of GA ranging from 0 to 10 M%: (A) 50 °C (phase I); (B) 80 °C (phase II). Dashed spectra are simulations based on Tables I and II, respectively.

Since an increase in water content increases the fluidity, we may expect that at higher water content the hardening feature (2) will be more important relative to the disordering feature (1), so the ordering would increase with increasing [P]. This is confirmed in Figure 14, where the ESR spectra from 16PC and 5PC in DPPC dispersions with excess water in the liquid crystalline phase are shown. It is most evident in the spectra from 5PC where the d value is found to increase from 13 to 15 G by addition of 2 M% GA, while for 16PC, given its low ordering, there is an extra broadening of the high-field line due to the unresolved splitting. Thus, though these spectra are also of the single-component type, they exhibit the opposite trend in ordering vs. [P] than the low-water-content samples.

Another use to which the spectra of Figure 13A can be put is to a consideration of the director-disorder model referred to above.
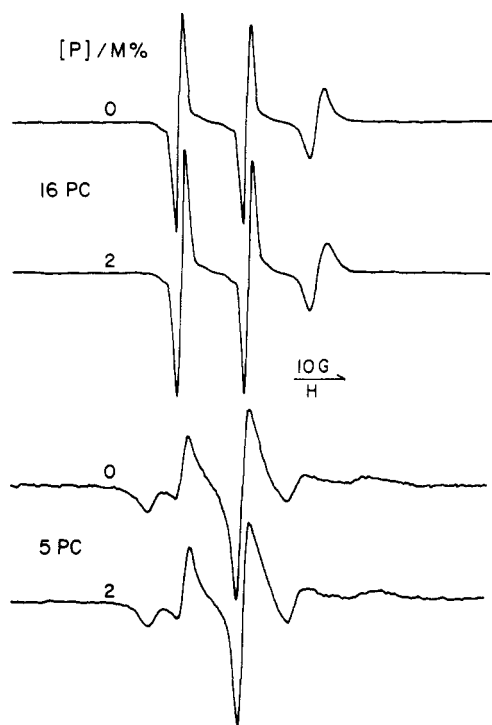
Figure 14. ESR spectra for 16PC and 5PC in unoriented DPPC dispersions in excess water for concentrations of GA of 0 and 2 M%. The temperature is 50 °C corresponding to the liquid crystalline phase.

If we assume that the disordered component has the same molecular ordering and dynamic properties as the ordered component, but only its preferred direction of orientation is randomized, then the disordered component becomes formally equivalent (as far as its spectrum is concerned) to the MOMD model. Thus, in a dispersion sample, the spectrum from the submicroscopically disordered regions and the MOMD spectra from the aligned regions which are now *macroscopically* disordered would be identical. Then the observed spectrum from dispersions would be independent of [P]. Figure 13A clearly shows that this is not so. Thus, even a director-disorder model would require significant changes in molecular ordering (and possibly dynamics) if it were to fit the observations.

When we examine Figure 13A closer we observe that a new feature appears in the dispersion spectrum as [P] increases that was not seen in the spectra from the oriented samples, and which is not predicted by the simulations. This is the appearance of new peaks substantially upfield and downfield from the main spectrum. They can most clearly be seen in the 10 M% spectra, and they appear to represent the growth of an immobilized species. It is clear that these new features are in no way associated with the disordered or ordered components observed in the oriented samples. Another model, that of microscopic order but macroscopic disorder (MOMD), has been proposed as an alternative to the growth of an immobilized species,[7] but it is not obvious that it could adequately predict these new features in Figure 13A.

When the water content is increased to 12 wt % in dispersion samples, we find that these new features in the ESR spectrum are sufficiently reduced that they tend to disappear below the noise level. Furthermore, there is no indication of such peaks even for 7 wt % water in phase II (cf. Figure 13B). Thus, they seem to be primarily characteristic of the low-water-content crystalline phase for which it follows from our above discussion that the disordering feature of GA should apply, and this would be appropriate for the MOMD model (while a model of immobilized species would be explained in terms of the hardening feature).

Perhaps the most interesting aspect is the fact that no hint of this extra structure was observed in the oriented spectra of 4 M% GA (cf. Figure 6A), for which a weak signal of this type should have been noticeable. The possibility emerges that perhaps the well-aligned lipid multibilayers do not permit the existence of such

immobilized lipids. We can cite a few examples in the literature indicating that aligning the lipid sample into multibilayers leads to changes at the molecular level, in the ordering and dynamics of certain spin probes.[20] It could be that only in the nonaligned dispersions can the GA molecules trap between them and immobilize some lipids.[1,12] One should also recall from section B that we observed a preference of GA molecules for the unoriented regions in samples that were only partially aligned.

We have also examined dispersion samples of CSL at low water content (7 wt %) and in excess water using very high concentrations of GA, i.e., [P] < 50 M%. For 7 wt % (at 50 °C in the gel phase I) extra peaks are clearly visible for [P] > 10 M%, but at 70 °C (phase II) they begin to emerge only for [P] > 20 M%. For excess water (at 30 °C in the gel phase) such peaks again appear only for [P] > 20 M% and may also be observed for these same high values of [P] in the liquid crystalline phase at 70 °C. Thus, in general, low fluidity (i.e., low water content and low temperature) favors the formation of such an immobilized species, and for high fluidity, extremely high [P] is required to generate them. However, many of the types of spectra obtained in these cases can be successfully generated by the one-site MOMD model.[7]

IV. Further Aspects of the Effect of GA on the Bilayer

The principal new observation in this work is the heterogeneity, on the molecular level, induced by GA in the gel phase (phase I). We estimate for 7 wt % water that there are about 30–40 disordered lipid molecules per GA (for [P] < 2 M%, cf. Table I and Figure 12), and this number is increased by reducing the water content to 3 wt % (cf. Figures 1 and 2 and Table I), while it is approaching zero at 17 wt % (cf. Figure 11). The role of the GA appears to be about the same in both the well-aligned multibilayers and the dispersions in this phase given that the parameters of Table I fit both types of specta (cf. Figures 6A, 7A, and 13A and for the moment we are ignoring the extra features in Figure 13A). If we therefore assume that each GA dimer is well intercalated into a bilayer, and use the estimate that about six lipid pairs can pack around a single GA dimer,[1,12] then for 7 wt % water the disordered region extends radially to a distance of about three lipid molecules in the bilayer (i.e., first, second, and third neighbors in hexagonal packing) or a radius of ca. 30 Å. As one proceeds further from the GA, the lipids are only weakly perturbed in phase I. However, the second important observation is that the motional rates of the disordered lipids are not significantly affected by the presence of the GA. That is, they are free to reorient with only a small reduction in diffusion coefficients. It is only the mean orienting potential, relative to which the motion occurs, that is dramatically influenced by the presence of GA. One might argue that in this phase the lipids around the helical GA are forced to take on orientations relative to this helix that minimize the packing constraints, and this tends to randomize their orientations relative to the main bilayer normal. On the other hand, the well-aligned bulk lipids tend to force those lipids at the edge of the disordered region to align properly. It would thus be the competition of the "boundary effects" on the GA vs. the transmission of alignment from the bulk lipids that would lead to the observed disorder. The model of molecular disorder would imply that this competition leads to a net molecular mean field in the disordered region which is greatly reduced, while the model of director disorder would imply that the mean field in the disordered region may not necessarily be significantly reduced, but is preferred direction of alignment would be nearly randomized. We have already pointed out (cf. section IIIG) that the model of molecular disorder is a better first approximation to our observations.

Actually, the molecular-disorder model should imply a distribution of ordering parameters as a function of radial distance from GA, although we have not included such a distribution in

(20) (a) E. Meirovitch and J. H. Freed, *J. Phys. Chem.*, **84**, 3295 (1980); (b) E. Meirovitch, *ibid.*, **87**, 845 (1983).

our simulations. As water is added, and the bilayer "softens", the radius of the disordered region may be expected to decrease, consistent with our observations that the number of disordered lipids is reduced.[21] In summary, the boundary effect of the GA is one of alignment (or more properly misalignment) and not of fluidity.

In the liquid crystalline phase II, we may expect reduced effects from GA due to a shorter coherence length. In fact the mean values of $\langle D_{00}^2 \rangle$ calculated for phase I (From Table I) show a greater relative rduction as a function of [P] than do the values given in Table II. We suspect that in phase II we are seeing an average spectrum from lipids translating rapidly enough between "boundary" and "bulk" regions,[22] but we cannot distinguish such a possibility purely by the observed ESR spectra from the alternative of a uniform lipid phase whose properties are significantly altered by addition of GA. The former does seem, on physical grounds, more consistent with the observations on phase I.

In the weakly aligned, high-temperature phase III, the GA helps to improve alignment of the lipids. This "hardening" effect is somewhat consistent with a model of Jähnig[21,23] who proposed that the ordering at the boundary of a protein should be lower than that for the "ordered" phase but greater than that for the "fluid" phase. While he had the main phase transition at T_c in mind, our low-water-content results are consistent with this model when we compare it instead with the II–III phase transition, which we previously characterized[10] as an "orientational order" transition. (Note, however, that for 4 M% GA $\langle D_{00}^2 \rangle$ for CSL is actually higher in phase III than in phase II!) For high-water-content dispersions this hardening effect is observed in the liquid crystalline phase.

Unlike previous ESR studies on dispersions, we see no sign of any immobilized component in our spectra from the well-aligned samples. Such a component is a characteristic of samples with very small lipid to protein (or polypeptide) ratios. We believe that our 2–4 M% GA samples are at least in that sense more representative of biological membranes. Our results, mainly for low water contents, indicate that GA does not immobilize lipids appreciably. Is GA a good model in this respect for protein–lipid interactions? This must await comparable studies with oriented samples containing proteins. However, we do note that when appreciable GA concentrations of >20 M% are reached in high-water-content dispersions, then such samples can also yield the immobilized features in the ESR spectrum that are commonly observed in the portein–lipid studies.[7] At such high concentrations of protein or polypeptide, the "trapped-lipid" model of Chapman[1,12] may be a likely explanation of immobilization, but it should not be of much significance at the low [P] we studied with our aligned samples. In fact, we have discussed preliminary evidence that such immobiliized species are not present in well-aligned samples,

which could imply that aggregation of GA molecules is inconsistent with macroscopic alignment.[24]

Another feature of the addition of GA is that the two-phase range of the I–II transition is broadened and shifted to high temperature. This has been observed by Chapman in his calorimetric work,[12] and we have also found it to be true in our ESR observations. Thus, in work at very high [P], one might expect a very broad two-phase region such that small amounts of a second phase are present far from the nominal phase transition. Perhaps the trapped or immobilized lipids seen in dispersions with very high [P] are due to persistence of a gel phase component in the L_α phase? In any case, we feel that a careful distinction between two types of lipid in a single phase vs. the presence of two phase regions has not been adequately considered in ESR studies. In our work we have taken considerable pains to distinguish between the two as we have discussed above.

V. Conclusions

(1) It has been possible to produce macroscopically well-aligned lipid samples of low water content (wt % $H_2O \leq 10\%$) containing GA up to 4 M%, which yield reproducible ESR spectra.

(2) The ESR spectra from such samples provide much greater detail on the molecular ordering and dynamics of the spin-labels than do dispersion samples. This permitted a quantitative assignment of the relevant parameters from theoretical simulations of the observed spectra.

(3) In the gel phase distinct two-component spectra could be assigned to highly oriented bulk lipids and to a disordered component that was fitted by a model of molecular disorder such that the ordering of these molecules is greatly reduced but its rotational-motional properties are not appreciably changed. The disordered region at lowest concentration of GA is estimated to consist of about 30–40 lipid pairs or about 2 times the number required to coat the GA dimer. This effect of disordering is significantly reduced by increasing the weight percent of water, but appears to be independent of temperature.

(4) In the liquid crystalline phase, heterogeneity is not distinguished from the ESR spectrum. Instead, the primary effect of GA is to significantly reduce the observed ordering of all the lipids, with only a very small decrease in motional rates. However, in the high-temperature weakly ordered phase, addition of GA actually leads to significant increase in ordering. This increase in ordering is also observed in high-water-content dispersions in the liquid crystalline phase. These effects are interpreted in terms of two competing features of the lipid–GA interaction: the disordering vs. the hardening feature.

(5) There is no hint of features usually assigned to immobilized species in any of the spectra obtained from well-aligned samples. However, such features are present in dispersion samples of 4 M% GA prepared from the same materials as the well-aligned ones. If these spectral features are associated with trapped lipids due to aggregation of GA, then it follows that microscopically well-aligned samples do not allow for such aggregation.

(6) The primary lipid–GA interaction is a disordering (or ordering) boundary effect and not one that appreciably affects fluidity.

(21) In a simplified Landau–de Gennes type of theory given by Jähnig [*Mol. Cryst. Liq. Cryst.*, **61**, 157 (1981)] the coherence length for distortions in $S = \langle D_{00}^2 \rangle$ caused by the boundary of a macromolecule is given by $\xi = \xi_0(2/a_2)^{1/2}$ where $a_2 = \Lambda[1-(2/15)(\Lambda M/(kT)^2)]$ with Λ the mean field aligning energy on the lipid chain and M is the elastic force constant resulting from intramolecular interactions favoring stretched chains. Also ξ_0, of order of a molecular distance, relates to the inhomogeneous term in the free energy: $\Lambda \xi_0^2 (\nabla S)^2$, and the steric interactions have been ignored for simplicity in obtaining ξ. While this is undoubtedly too simple a model with which to analyze our results, we may comment that the above formula would predict that since $\xi \approx \xi_0/\Lambda^{1/2}$ decreases with added water, then the force constant $K \propto \Lambda \xi_0^2$ must decrease very rapidly with added water compared to any decrease in Λ.

(22) In fact for [P] $\geq$ 2 M% we find that the mean $\langle D_{00}^2 \rangle$ calculated from Table I for both 16PC and CSL are in almost *exact* agreement with the average values in Table II. (The relative change as a function of [P] is, of course, less in phase II, as stated above.)

(23) Other theoretical treatments of protein–lipid interactions in membranes include: J. C. Owicki, M. W. Springate, and H. M. McConnell, *Proc. Natl. Acad. Sci. U.S.A.*, **75**, 1616 (1978); J. C. Owicki and H. M. McConnell, *ibid.*, **76**, 4750 (1979); S. Marcelja, *Biochim. Biophys. Acta* **455**, 1 (1976); D. Pink and D. Chapman, *Proc. Natl. Acad. Sci. U.S.A.*, **76**, 1542 (1979); M. Tessier-Lavigne, M. A. Boothroyd, M. J. Zuckerman, and D. A. Pink, *J. Chem. Phys.*, **76**, 4587 (1982); O. G. Mouritsen and M. Bloom, preprint.

(24) Bienvenue et al. [A. M. Bienvenue, M. Bloom, J. H. Davis, and P. F. Devaux, *J. Biol. Chem.*, **257**, 3032 (1982)] do observe, by ^{2}H NMR on dispersions of DMPC-d_{54} reconstituted with rhodopsin below T_c, spectra that they interpret in terms of two components: a pure phospholipid gel phase spectrum and another nongel type they attribute to lipids in protein aggregates. They estimate there are 30 lipids of the nongel type per protein, and this is close to the estimated number required to coat the protein. We suspect that such NMR observations on this high-water-content dispersion are more akin to our ESR observations that "immobilized peaks" appear for [P] $\geq$ 20 M% in the high-water-content gel phase (cf. above), rather than our observations on the low-water-content well-aligned samples.